Available free online at www.medjchem.com

Mediterranean Journal of Chemistry **2018**, 7(3), 204-216

Coriandrum Sativum seeds as a green low-cost biosorbent for methylene blue dye removal from aqueous solution: spectroscopic, kinetic and thermodynamic studies

Lamya Kadiri*, Abdelkarim Ouass, Youness Essaadaoui, El Housseine Rifi and Ahmed Lebkiri

Laboratory of Organic Synthesis and Extraction Processes - Department of Chemistry
University Ibn Tofail, Kenitra - Faculty of Sciences, PO Box. 133 – 14000- Morocco

Abstract: Coriandrum sativum seeds (CSS) were investigated as a new eco-friendly and economic biosorbent for the removal of methylene blue (MB) dye from synthetic solutions. First, the spectroscopic analyses were effectuated using FTIR and SEM to confirm the possibility of CSS to remove MB dye from aqueous solutions. The study of the influence of different parameters, such as contact time, CSS mass, solution pH, MB concentration, and temperature was realized and proved the rapid and efficient power adopted by CSS as a removal of the studied dye. Also, the regeneration study was effectuated for four cycles with excellent adsorption rates. The modeling studies revealed that the studied process obeys the pseudo-second-order model and Langmuir isotherm model. The adsorption amount was found to be 107.53 mg/g. Finally, the determination of thermodynamic parameters indicated the exothermic and spontaneous type of the removal process of MB onto CSS.

Keywords: Coriandrum Sativum, biosorption, Methylene blue dye, FTIR, SEM, kinetic, thermodynamic, isotherm.

Introduction

Last decades, industries have produced various kinds of toxic pollutants such as dyes, heavy metals, and pesticides, which cause serious and dangerous health problems to living species, even to human health [1]. In consequence, different national and international agencies have created strict regulations on the manufacture and use of synthetic colorants in several domains such as textile, paper, paints, and plastics. Pigment and dye industries have given importance to develop novel technologies to analyze and remediate dyes in wastewater. Therefore, big efforts must be done in order to provide an organized and comprehensive treatment of the environmental chemistry of synthetic colorants [2].

In the area of wastewater treatment, several techniques have been investigated to combat pollution issues, especially dyes removal from wastewaters including ion exchange, precipitation, ultrafiltration, reverse osmosis and electrodialysis. However, adsorption is preferred for dyes removal due to easy handling, low cost strategy and removal performance [3-6].

In fact, the exploration of natural adsorbents which can eliminate dyes from aqueous solutions is an essential field of research due to being environmentally friendly and ecologically acceptable. Many natural substances have been used in this context, such as macroalgae [7], biochars [8], rice straw [9], *Cucumis Sativus* [10], carica papaya [11], fly ach [12], and cactus [13].

Coriander (coriandrum sativum) is a popular spice [14] and a major ingredient of curry powder, an effective antioxidant [15] and a drug for rheumatism, against worms, and indigestion [16]. Coriander seeds have also many properties as antimicrobial activity [17], insecticidal effect, hypolipidemic activity [18], hypoglycemic action [19], corrosion inhibition [20], and adsorption of heavy metals [21].

The purpose of the present study is to investigate the effect of coriandrum sativum seeds (CSS), after its characterization [22], as a removal of methylene blue (MB) from contaminated solutions since its adsorption potential hasn't been previously reported. The study of the effect of several parameters has been effectuated. The adsorption isotherms and thermodynamic studies have been also established and discussed. The characterization of CSS using FTIR and SEM techniques has been realized to confirm all previous studies.

**Corresponding author: Lamya Kadiri*
Email address: kadiri.lamya@gmail.com
DOI: http://dx.doi.org/10.13171/mjc731810911-kadiri

Received September 7, 2018
Accepted September 24, 2018
Published October 9, 2018

Material and Methods

Preparation of adsorbent

The coriander seeds (Coriandrum Sativum) were collected from the west of Morocco (Kenitra), washed with double distilled water to remove impurities such as sand and dust, dried in air at 50 °C for 24 hours, ground using mortar, and then sieved, until the grain-size of particles was lower than 250 µm. The obtained powder was washed with double distilled water and filtrated consecutive times in order to acquire a clean powder. The resulted material was stored in a desiccator to prevent it from humidity [21, 22].

Preparation of aqueous solution

Synthetic solutions were prepared from methylene blue powder (purchased from Sigma Aldrich). The stock solution (1g / L) was then used to obtain the working solutions through dilution with double distilled water. Fresh dilutions were made and used for each experiment. 10^{-1} mol /L HCl or NaOH solutions were used to control the solution pH of aqueous solutions.

Structure and chemical properties characterizing the studied methylene blue were illustrated in (Table 1)

Table 1: Chemical properties of Methylene blue.

Properties	Methylene Blue
Chemical formula	$C_{16}H_{18}ClN_3S$
λ_{max}	664.5 nm
Structure	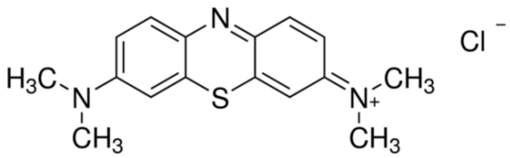
Toxicity	Anemia Nauses, vomlting, diarrhoea Discoloration of urine Dizziness, headache, fever

Adsorption experiments

The extraction experiments were realized through the batch method, CSS dose was added to 100 mL of aqueous solution with known MB concentration, in several 200 mL conical flasks. Each flask was intermittently stirred for an adequate period of time, depending on the experiment purpose. All experiments were studied at room temperature (25°C) [23]. After adsorption experiments, samples were placed in a laboratory centrifuge (Hettich Zentifugen, EBA 200) with a rotation speed 5000 for 5 min in order to separate the adsorbent from MB solution, and then were analyzed using a UV-Visible spectrophotometer (Selecta P, Model UV-2005) at 664.5 nm.

Data evaluation

The adsorption process of MB by CSS was evaluated by calculating the removal rate and the amount of adsorption respectively using (Eq.1 and 2) from experimental results [24]:

$$R = \frac{C_0 - C_e}{C_0} * 100 \qquad (1)$$

$$Q_e = \frac{C_0 - C_e}{m} * V \qquad (2)$$

Where C_0 is the initial concentration of MB in the solution (ppm), C_e is the equilibrium concentration of MB in the solution (ppm), V is the aqueous solution volume (L), and m is the mass of coriander seeds (g). All the data represent the average values of three repeated measurements.

Results and discussion

Characterization of the adsorbent

Fourier Transformed Infrared analysis (FTIR)

To study the possible nature of CSS-MB interactions, and determine the various functional groups contributing in this interaction, FTIR analysis of CSS and CSS-MB was realized using a Perkin Elmer Spectrum apparatus version 10.03.07 ATR with the spectral resolution 4.0 cm^{-1}. Both of the corresponding FTIR spectra were shown in (Fig. 1). A strong peak at 3415.66 cm^{-1} indicates the presence of hydroxyl group. The presence of aliphatic groups ($-CH_2$ or $-CH_3$) was proved by the peak at 2925.96 cm^{-1} due to the stretching vibrations of C–H bonds. It can be clearly deduced that the decrease in peak size at 3416.57 cm^{-1} indicates the involvement of hydroxyl group in the CSS-MB interaction [23].

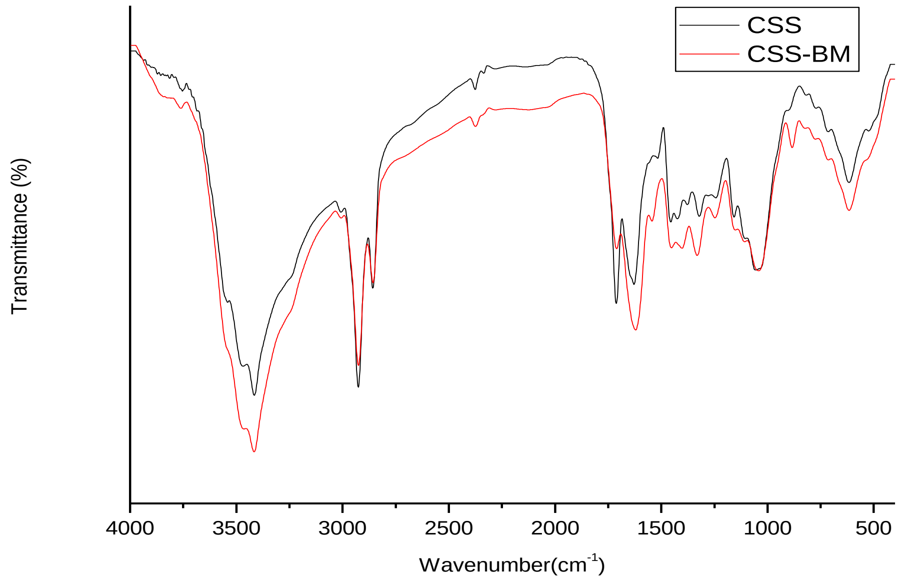

Figure 1. FTIR spectra of CSS before (a) and after (b) adsorption of methylene blue

Scanning Electron Microscopy analysis

The surface analysis has been effectuated using a Scanning Electron Microscope (SEM) model VEGA3 TESCAN. The obtained SEM micrographs of Coriandrum Sativum seeds before and after MB removal process have been illustrated in (Fig. 2), respectively. In fact, before adsorption experiments, CSS had a rough surface containing numerous cavities (Fig. 2a). However, these cavities were filled with MB dye in (Fig. 2b). It can be deduced that CSS can act as an excellent adsorbent of methylene blue [25].

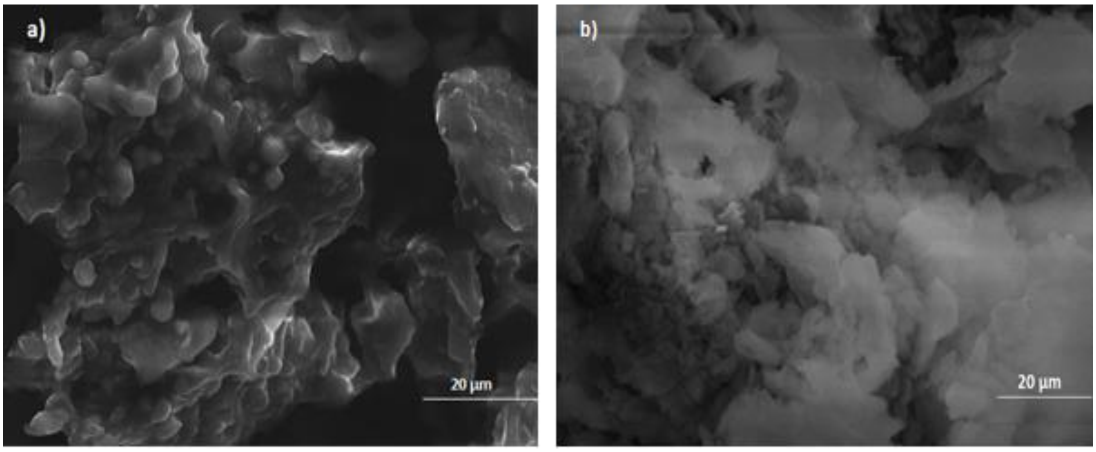

Figure 2. SEM micrographs of CSS before (a) and after (b) adsorption of MB

Effect of contact time

The influence of contact time on MB adsorption by coriander seeds, at room temperature (25 °C), constant adsorbent mass 0.1 g, solution pH of 5.5 and initial MB concentration 10 ppm, is illustrated in (Fig. 3). The experimental data indicate that the adsorption efficiency of the studied dye onto coriander seeds increases with the increase of contact time (ranging from 10 to 240 minutes), and reaches the maximum value 91.25 % after 25 min. These results can be attributed to the accessibility of vacant sites mentioned in FTIR analysis on the adsorbent surface from the beginning of the experiment to the equilibrium time when these sites have been occupied by MB [10].

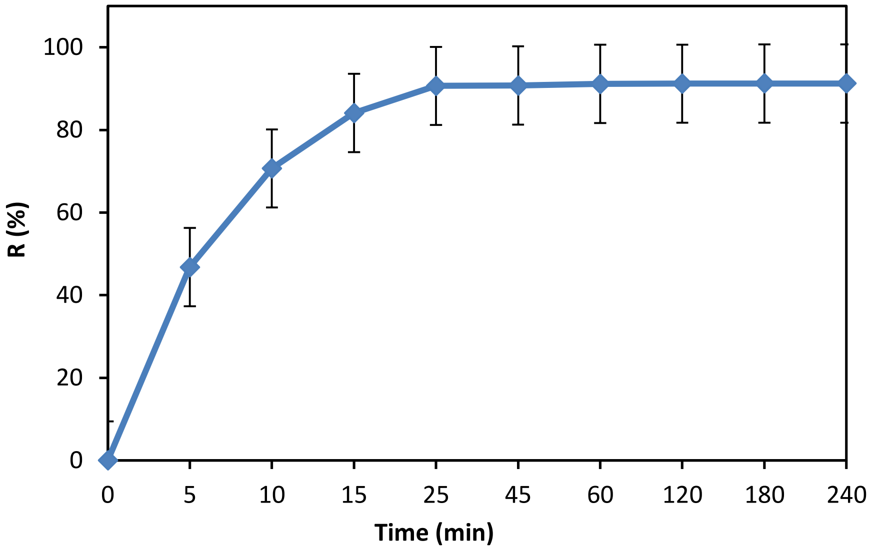

Figure 3. Effect of contact time on the adsorption rate of MB by CSS

Effect of adsorbent mass

The effect of adsorbent mass on the MB adsorption was tested through different quantities of coriander seeds and maintaining constant all other experimental parameters. The acquired results are presented in (Fig. 4). The experimental results showed that the removal rates increase with the increase of adsorbent mass. This rise of CSS weight from 0.02 to 1.0 g displayed an important improvement of adsorption efficiency from approximately 68.56 to 98.11 % owing to the more availability of the surface area [11]. The increase of the CSS dose over 0.2 g did not display an additional increase in the adsorption efficiency, probably due to the adsorption saturation. Therefore, for economic considerations, the optimum adsorbent weight was selected as 0.1 g.

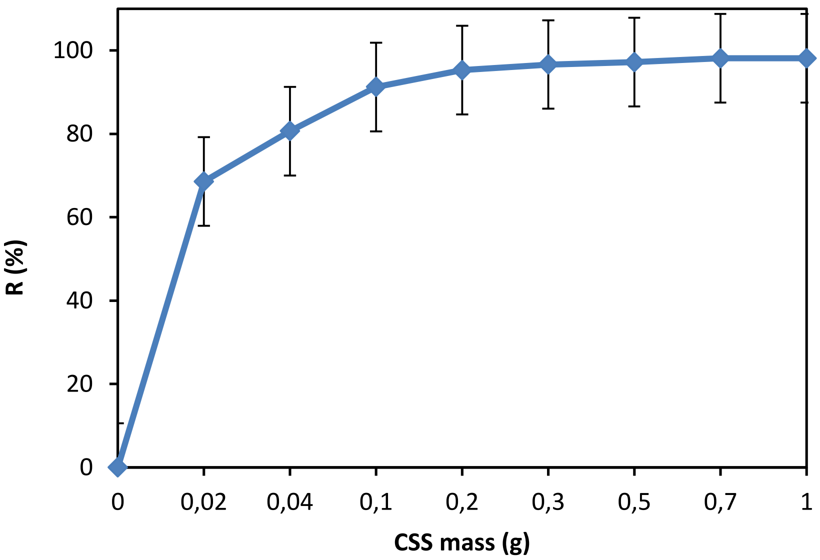

Figure 4. Effect of adsorbent mass on the adsorption rate

Effect of solution pH

The effect of the solution pH on the adsorption efficiency of MB dye by Coriander seeds was studied in the pH interval between 2 and 12 (Fig. 5), at a constant MB concentration 10 ppm, contact time (2h) with 0.1 g of CSS and room temperature of 25 °C. The point of zero charge, pH_{pzc} of adsorbent was determined. In brief, 100 ml of 0.01 M NaCl solutions were placed in various Erlenmeyer flasks. Their pH was adjusted to different values between 2 to 12 by the addition of 0.1 M HCl or NaOH solutions.0.1 g of adsorbent powder was added into each solution and the final pH of these solutions was recorded after 48 hours of agitation. The pH_{pzc} is the point where the curve pH_{final} verses $pH_{initial}$ intersects the straight line corresponding to:

$$pH_{initial} = pH_{final}$$

The point of zero charge value corresponding to CSS was determined from (Fig. 5) and found to be 6.23. The removal percentages increase when the initial solution pH increases from 2 to 12. In acidic medium (pH = 2.0), where pH is lower than $pH_{pzc,}$

CSS active sites were positively charged because of the highest number of protons existing in the aqueous solution and then the removal percentage is very low 8.51%. However, the increase in pH correlates with an increase of MB removal efficiency until a pH of 5. After that point, the pH value become higher than pH_{pzc} one and the CSS functional groups in the surface were charged negatively, also the adsorption efficiency remains constant approximately at 93 % in spite of the pH increase [26, 27].

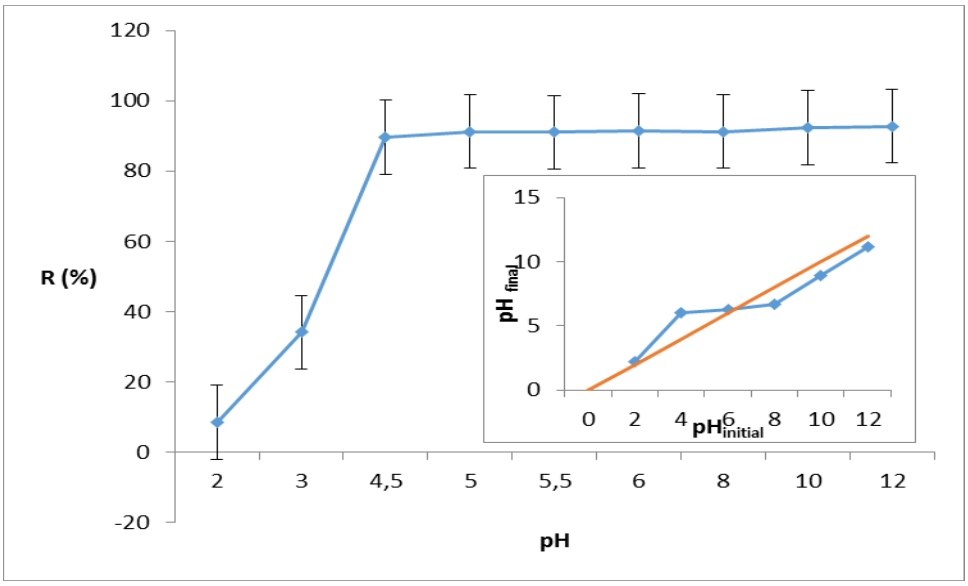

Figure 5. Effect of medium pH on the adsorption rate of copper by CSS

Effect of initial MB concentration

The effect of initial MB dye concentrations on the adsorption performances adopted by coriander seeds CSS, under optimum experimental conditions (0.5 g of adsorbent; initial solution pH of 5.5 and 2 hours of contact time) is illustrated in (Fig. 6). The study is carried out at several concentrations ranging from 10 to 300 ppm. It can be seen that the adsorption amount of MB by coriander seeds increases with the increase of initial MB concentration from 9.12 to 101.3 mg/g. This significant increase of the adsorption efficiency values is expected because high initial MB concentrations correlate with a higher driving force of concentration gradient and a higher probability of collisions between MB cationic molecules and superficial functional groups negatively charged of the adsorbent [28].

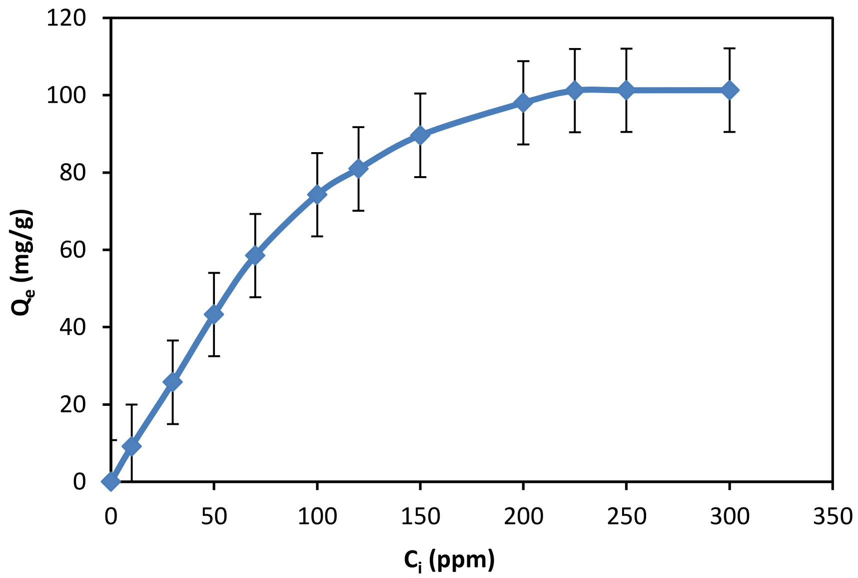

Figure 6. Effect of initial concentration of MB on the amount of adsorption

Effect of temperature

The effect of temperature on MB adsorption amount by CSS was also studied. Four different temperatures of 298, 308, 318 and 328 K were considered. From (Fig. 7), the obtained removal rate of MB by coriander seeds decreases from 91.03 % to 77.01 %, when the temperature changes from 25 to 55 ° C, respectively. These results indicate that the dye adsorption process may be exothermic and can be described out by the fact that the rise in temperature may not be in favor of any agglomeration of MB on the solid surface [29].

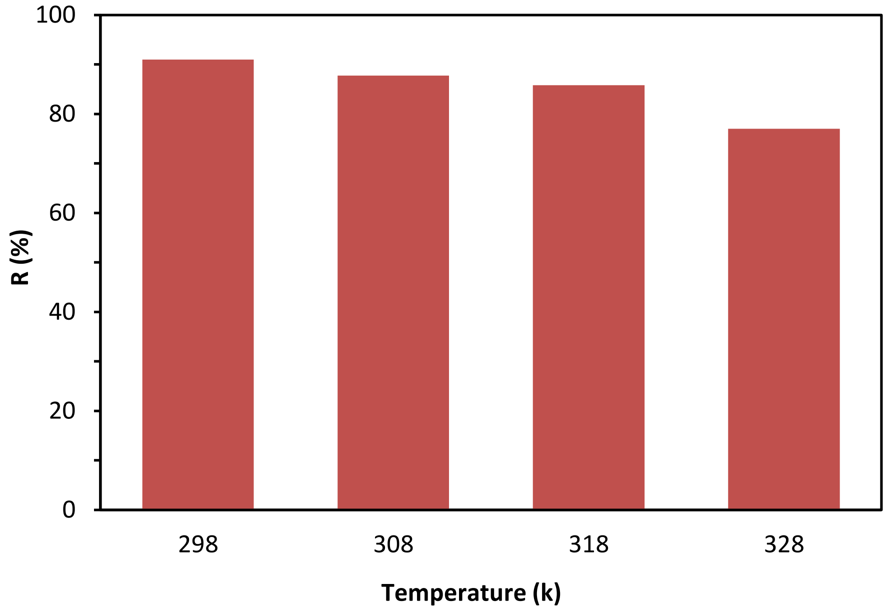

Figure 7. Effect of temperature on the adsorption of MB by CSS

Desorption study and regeneration study

Concerning desorption experiments, the adsorbent sample resulted through the study of the effect of contact time was separated by filtration. The adsorbent samples loaded with MB dye were treated with 25 mL of 0.1M HCl, CH_3COOH, NaOH, and NaCl solutions, and then intermittently stirred for 10 min. A sample was recuperated after each minute. After filtration, the equilibrium desorption rate of MB dye was determined for each reagent and represented in (Fig. 8).

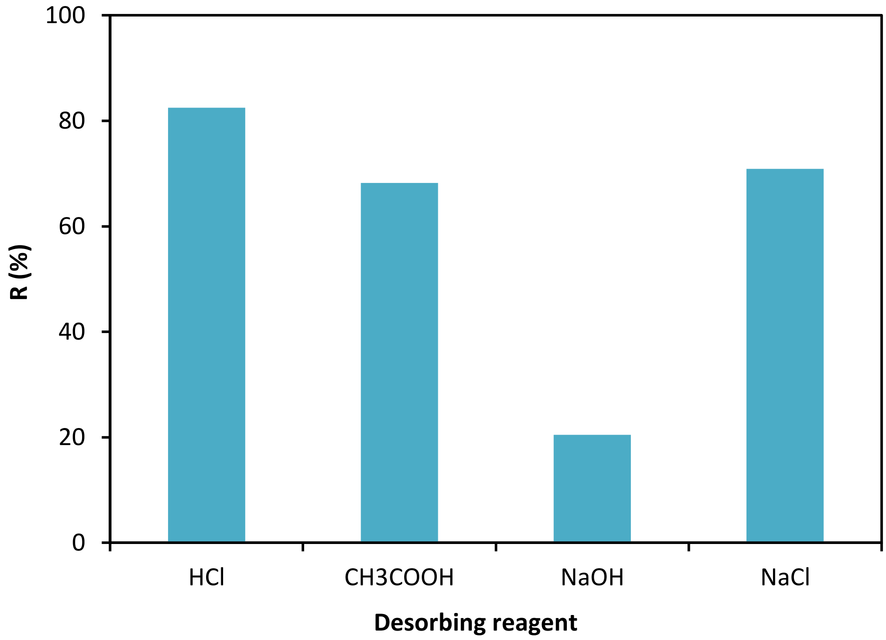

Figure 8. Desorption of MB dye from CSS using different desorbing reagents

It is clear from the Fig 8 that hydrochloric acid is the most effective medium (82.5 %) while the sodium hydroxide is the worst medium (20.5 %) for desorption of MB from CSS. It can be attributed to the fact that the product CSS-MB has reacted with HCl solution by releasing MB and fixing protons on CSS surface, while the basicity of NaOH has prevented CSS-MB from desorption of MB.

Recyclability of an adsorbent is very important in industrial practice for pollutants removal from wastewaters. To test the suitability and stability of the adsorbent, it was necessary to successive adsorption and desorption cycles [30]. The procedure was carried out four times and 25 mL of 0.1 M HCl was used as the elution solution. The adsorbent was washed with water before each measurement. The results have been represented in (Fig. 9) and have clearly shown that CSS can be used repeatedly four times without significantly losing the adsorption efficiency for MB. The regeneration efficiency indicates that the sorbent is suitable for commercial use [31].

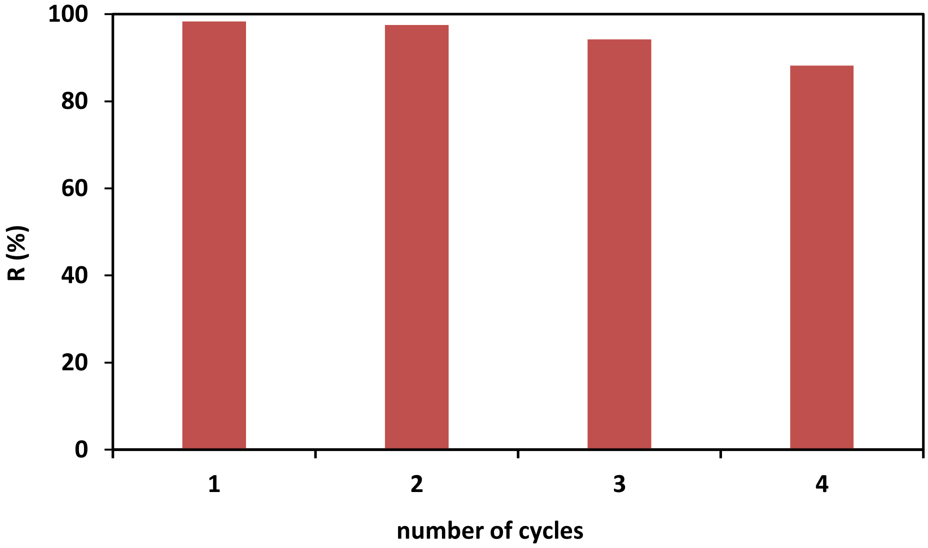

Figure 9. Four (Adsorption / desorption) cycles using 0.1M HCl

Adsorption kinetics

The experimental data of MB adsorption on CSS were investigated using Lagergren pseudo first order and pseudo second-order models.

- Lagergren pseudo-first-order:

The experimental measurements were analyzed using linear form of Lagergren pseudo-first order (Eq. 3):

$$\log(Q_e - Q_t) = \log(Q_e) - \frac{K_1}{2.303}t \qquad (3)$$

Q_e is the equilibrium amount of adsorption (mg/g), Q_t is the amount of adsorption of CSS at time t (mg/g) and K_1 is the rate constant (min^{-1}).

The pseudo-first-order model corresponding to the adsorption of MB on CSS is shown in (Fig. 10).

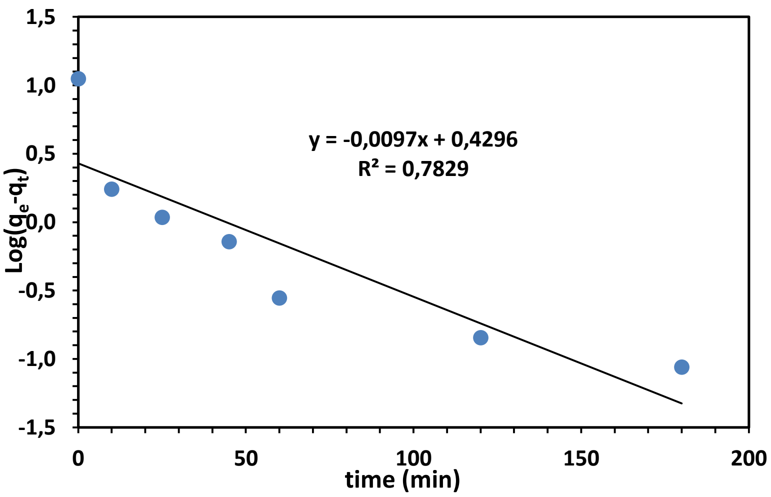

Figure 10. pseudo first-order model

- Pseudo-second order:

The pseudo-second-order kinetic model is expressed in the linear form as the following (Eq. 4) [32]:

$$\frac{t}{Q_t} = \frac{t}{Q_e} + \frac{1}{(K_2.Q_e)^2} \qquad (4)$$

Q_e is the equilibrium amount of MB adsorption (mg/g), Q_t is the amount of adsorption of CSS at time t (mg/g) and K_2 is the rate constant ($g.mg^{-1}.min^{-1}$). The pseudo-second-order model is shown in (Fig. 11).

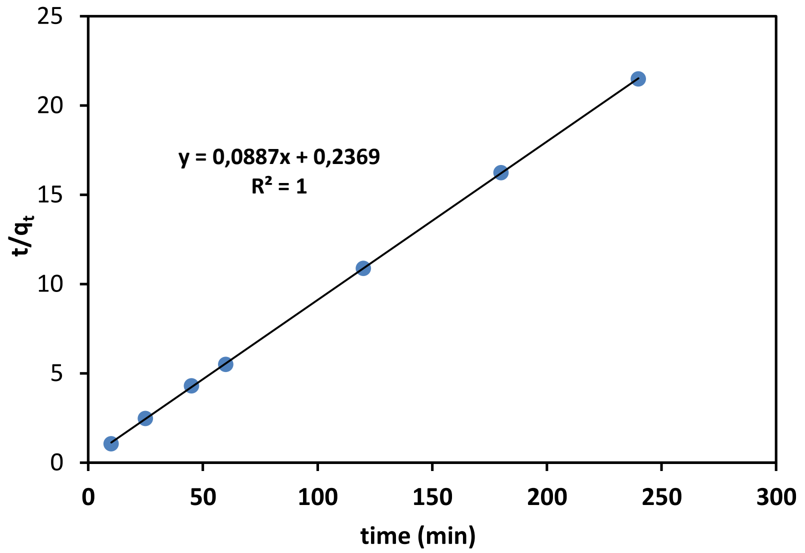

Figure 11. Pseudo-second order model

(Table 2) has represented the reported parameters characterizing both of Lagergren models (pseudo first order and pseudo second order) obtained from (Figs. 10 and 11).

Table 2. Parameters of adsorption kinetic models.

Kinetic model	Parameters				
Pseudo-first order	$q_{e\,;\,exp}$ (mg.g^{-1})	$q_{e\,;\,calcul}$ (mg.g^{-1})	DR%	k_1 (min^{-1})	R^2
	11.17	2.7	313	0.022	0.7829
Pseudo-second order	$q_{e\,;\,exp}$ (mg.g^{-1})	$q_{e\,;\,calcul}$ (mg.g^{-1})	DR%	k_2 (min^{-1})	R^2
	11.17	11.27	0.8	0.033	1

According to Table 2, the determination coefficient R^2 values corresponding to pseudo-second-order model of adsorption process at different concentrations are equal to unity, also the relative difference between the experimental and calculated values of adsorption amount DR (%) are very low in comparison with pseudo first-order ones which confirms that the adsorption of MB by CSS from aqueous solution followed the pseudo-second-order model [33]. It was clear that the rate constant of the pseudo-second-order model decrease gradually with the increase of MB concentration. All results can be due to competition between higher levels of MB and CSS active sites. In fact, k_2 values suggest that adsorption systems with low concentrations have required a short time to achieve a specific fractional uptake. To sum up, the adsorption process may be a chemisorption type involving valent forces through sharing or the exchange of electrons between the peat and divalent metal ions [34].

Adsorption isotherms

The isotherms models are applied for analyzing adsorption equilibrium results through experiments and studying the surface properties of the adsorbent and its affinity for an adsorbate.

- Langmuir model

The model supposes that maximum adsorption occurs when a saturated monolayer of molecules from aqueous solution is present on the adsorbent surface and the energy of adsorption is constant and there is no migration of absorbate molecules in the surface plane [35]. The linear form is expressed by (Eq. 5):

$$\frac{C_e}{Q_e} = \frac{1}{K_L Q_m} + \frac{C_e}{Q_m} \qquad (5)$$

C_e is the concentration value of MB at equilibrium, Q_e is the amount of adsorption (mg/g) at equilibrium, Q_m is the maximum amount of adsorption (mg/g) and K_L is the Langmuir constant which related with the affinity of the binding sites (L/g). The fitting line which represents the Langmuir isotherm model is shown in (Fig. 12).

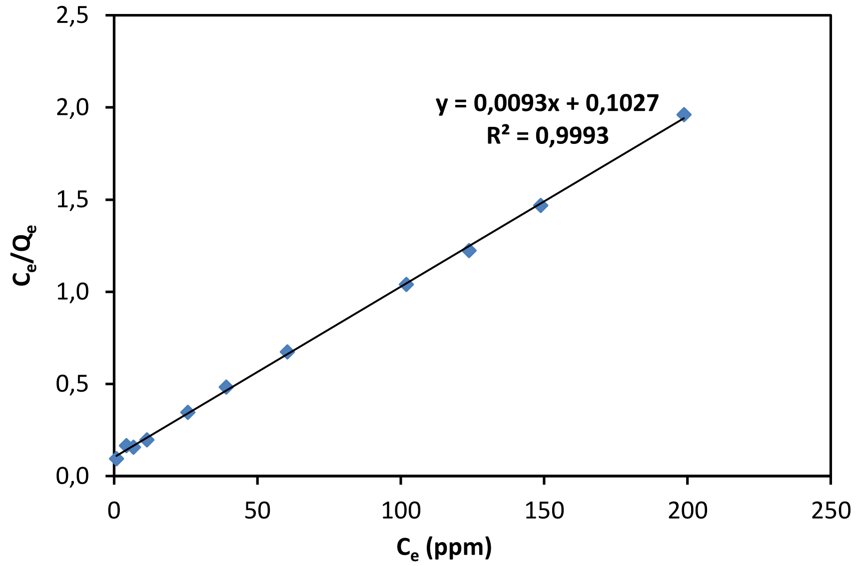

Figure 12. Langmuir isotherm model

The important characteristic of this model dimensionless constant separation factor R_L can be calculated through (Eq. 6):

$$R_L = \frac{1}{1 + K_L C_0} \quad (6)$$

Where C_o is the highest concentration of the adsorbate (mg/L), and K_L (L/mg) is Langmuir constant. The value of R_L indicates the shape of the isotherm to be either unfavorable ($R_L > 1$), linear ($R_L = 1$), favorable ($0 < R_L < 1$), or irreversible ($R_L = 0$) [36].

- Freundlich

The Freundlich equation at the linear form that is often applied to adsorption on heterogeneous surfaces as well as multilayer adsorption is given by (Eq. 7) [37]:

$$\log(Q_e) = \log(K_F) + \frac{1}{n} \log(C_e) \quad (7)$$

Q_e is the amount of adsorption (mg/g) at equilibrium, K_F is the Freundlich constant (L/g), and C_e is the concentration value of MB at equilibrium. The magnitude of the exponent, $1/n$, proves the favorability of adsorption, $n>1$ signifies favorable adsorption condition. K_F and n values are obtained through the intercept and slope of the Freundlich plot represented in (Fig. 13) and listed in Table 3.

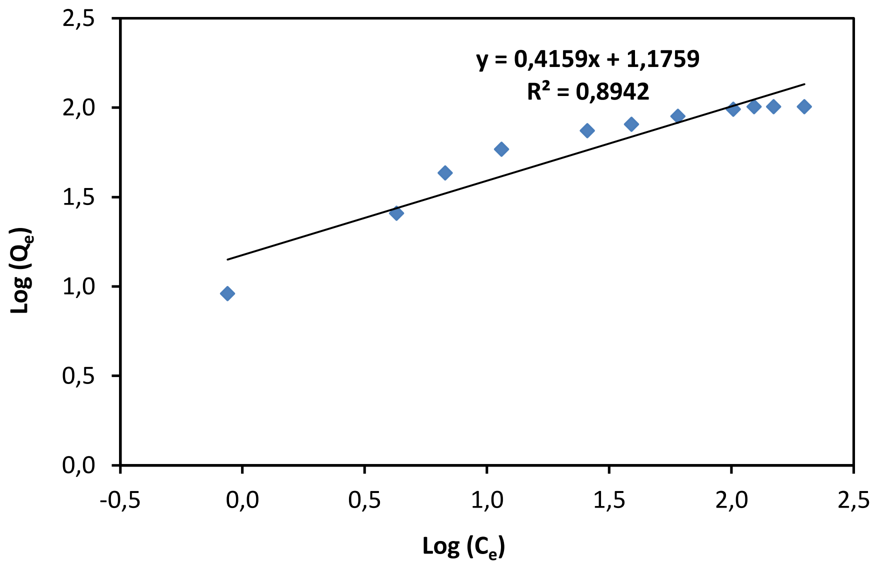

Figure 13. Freundlich isotherm model

- Dubinin Radushkevich

The Dubinin Radushkevich isotherm has generally been applied in the linear form as following (Eq. 8) [38]:

$$\ln Q_e = \ln Q_m - B\left(RT \ln\left(1 + \frac{1}{C_e}\right)\right)^2 \quad (8)$$

Where Q_e is the amount of adsorption (mg/g) at equilibrium, Q_m is the maximum amount of adsorption (mg/g), R the gas constant (8.314 J/mol.K) and T the absolute temperature (K). Therefore, by plotting ln Q_e versus $RT \ln\left(1+\frac{1}{C_e}\right)$ in (Fig. 14), the constant B consequently can be determined and then listed in (Table 3).

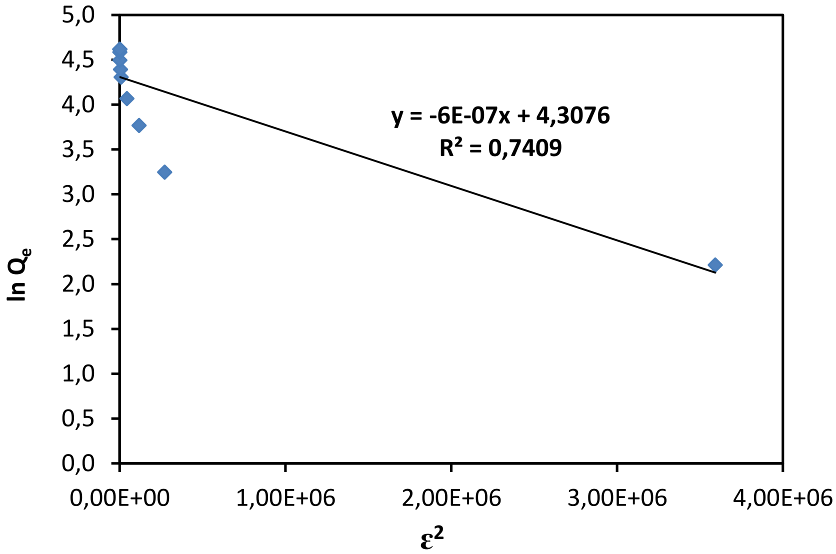

Figure 14. Dubinin Radushkevich isotherm model

(Figs. 12, 13 and 14) have shown respectively the Langmuir, Freundlich and Dubinin Radushkevich adsorption isotherms corresponding to the removal of MB dye by CSS at 298 K. All parameters characterize each isotherm model that has been represented in (Table 3). According to the obtained values, all models describe the adsorption process. All plots have a good linearity in all the cases. The values of the determination coefficients indicate the favorable nature of adsorption of MB dye on CSS. According to results represented in (Table 3), the biosorption obeys Langmuir model which assumes monolayer coverage of MB dye over the homogeneous surface of CSS [39], and the adsorption of each molecule onto the surface has the same adsorption activation energy.

Table 3. Adsorption isotherm model parameters.

Isotherm Models	Parameters	
Freundlich	K_F (mg.g^{-1})	15
	n	2.4
	R^2	0.8942
Langmuir	q_m (mg/g)	107.53
	q_m exp (mg/g)	101.3
	K_L (L/mg)	0.091
	R_L	0.035
	R^2	0.9993
Dubinin Radushkevich	B (mg/g)	6.10^7
	R^2	0.7409

Thermodynamic studies

Thermodynamic study is necessary for an adsorption process to describe the process (type, spontaneity…). All corresponding parameters as free energy (ΔG^0), enthalpy (ΔH^0), and entropy (ΔS^0) changes can be estimated using equilibrium constants changing as a function of temperature [40].
ΔG^0 is the standard free energy change (J) is calculated by (Eq. 9) [41,42]:

$$\Delta G^0 = -RT \ln (K_D) \tag{9}$$

R is the universal gas constant (8.314 J/mol K) and T is the room temperature (298 K) and K_D is the thermodynamic equilibrium constant (L/g) that can be expressed as (Eq. 10):

$$K_D = \frac{Q_e}{C_e} \tag{10}$$

Where Q_e (mg/g) is the amount of MB dye adsorbed at equilibrium, C_e (mg/L) is the concentration of MB at the system equilibrium. The values of ΔH^0 and ΔS^0 were determined from the slope and the intercept of ln (K_D) versus 1/T (Figure 15) by (Eq. 11):

$$\mathrm{Ln}\,(K_D) = -\frac{\Delta H^0}{RT} + \frac{\Delta S^0}{R} \tag{11}$$

ΔG^0, ΔH^0, and ΔS^0 are related by (Eq. 12):

$$\Delta G^0 = \Delta H^0 - T\Delta S^0 \quad (12)$$

The Van'tHoff plot which corresponds to the adsorption process of MB by CSS was illustrated in (Fig. 15).

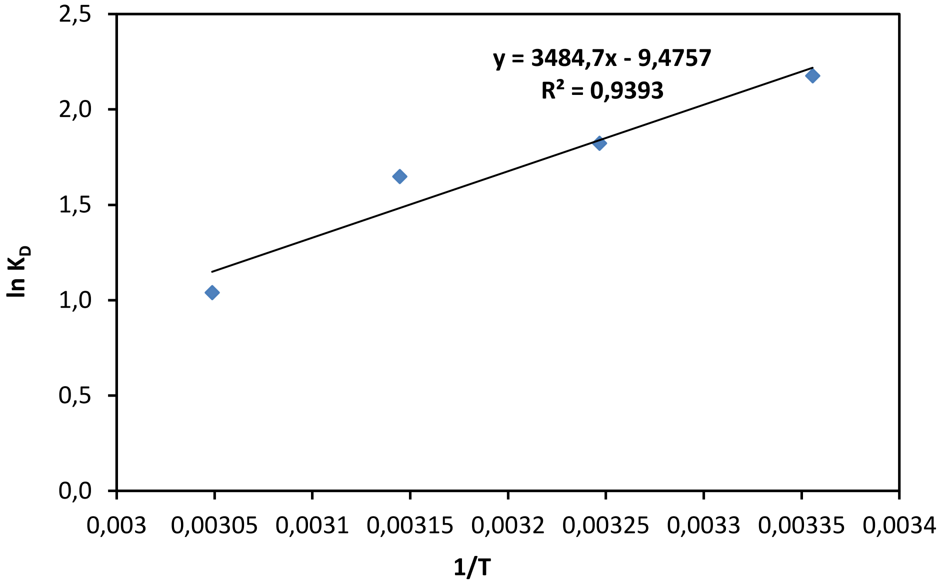

Figure 15. Van'tHoff curve corresponding to the adsorption of MB by CSS

The thermodynamic parameters were listed in (Table 4). The ΔH° value has confirmed the exothermic type process [43]. Also, ΔG° and ΔS° values have proved the stability, feasibility, and randomness of the adsorption process. In fact, these values imply that the retention process of MB dye by CSS is a combination of two mechanisms: ions exchange and adsorption.

Table 4. Thermodynamic parameters of the adsorption process.

Temperature (K)	K_D (L/g)	ΔG° (KJ/mol)	ΔH° (KJ/mol)	ΔS° (KJ/mol)
298	8.81	-5.401	- 28.97	- 0.078
308	6.19	- 4.660		
318	5.19	- 4.362		
328	2.83	- 2.836		

Comparison with other adsorbents

(Table 5) has shown various adsorbents that have been studied previously for the removal of methylene blue. It is found that the adsorption amount of Coriander seeds is among the highest capacities of natural adsorbents. All results are encouraging for testing CSS as a low-cost removal of methylene blue dye from industrial wastewaters.

Table 5. Comparative study of the extraction of MB by different materials.

Adsorbent	Adsorption capacity (mg/g)	Reference
Bivalve shell	1.00	33
Carica Papaya	32.25	11
Biochar	33	8
Salix Babylonica	60.97	23
***Coriandrum Sativum* seeds**	**107.53**	**Present work**
Abelmoschus esculentus	205.65	25
Almond gum	250	28

Conclusion

Coriandrum Sativum seeds were found to be an excellent removal of methylene blue dye from artificial solution. SEM and FTIR analysis have shown that CSS can remove MB dye from aqueous solution by adsorption process. The equilibrium was obtained for 25 min of contact time. Different parameters, which influence the adsorption process, have been studied such as adsorbent mass, pH, initial MB concentration and temperature. The kinetic measurements showed that the mechanism follows the pseudo-second-order model. The adsorption process was described by the studied kinetic isotherms models (Langmuir, Freundlich, and Temkin). The $\Delta S°$, $\Delta H°$ and $\Delta G°$ values obtained through the thermodynamic study indicate the exothermic, the stable and spontaneous nature of the adsorption process on the surface of CSS. The study revealed that this new adsorbent is inexpensive, indigenous, easily available material and can have an application for the removal of MB dye contained in industrial effluents.

Acknowledgment
The authors are pleased to acknowledge:
The Center of Analysis and characterization (C.A.C.) in Cadi Ayyad University, Faculty of sciences, Marrakech, Morocco, for their kindness.

References

1- L. Travieso, R. O. Canizares, R. Borja, F. Benitez, A. R. Dominguez, and V. Valiente, Heavy metal removal by microalgae, Bulletin of Environmental Contamination and Toxicology, **1999**, 62, 144–151.
2- A. Reife, A. Reife, H. S. Freeman, Environmental Chemistry Dyes and Pigments. John Wiley & Sons. **1996**.
3- S. S. Salih, T. K. Ghosh, Adsorption of Zn (II) ions by chitosan coated diatomaceous earth." International journal of biological macromolecules, **2018**, 106, 602-610.
4- S. S. Salih, T. K. Ghosh, Preparation and characterization of bioadsorbent beads for chromium and zinc ions adsorption." Cogent Environmental Science, **2017**, 3, 1401577.
5- S. S. Salih, T. K. Ghosh, Highly efficient competitive removal of Pb (II) and Ni (II) by chitosan/diatomaceous earth composite. Journal of environmental chemical engineering, **2018**, 6, 435-443.
6- S. S. Salih, T. K. Ghosh, Preparation and Characterization of Chitosan-Coated Diatomaceous Earth for Hexavalent Chromium Removal. Environmental Processes, **2018**, 5, 23-39.
7- E. Daneshvar, A. Vazirzadeh, A. Niazi, M. Sillanpää, and A. Bhatnagar, A comparative study of methylene blue biosorption using different modified brown, red and green macroalgae – Effect of pretreatment, Chemical Engineering Journal, **2017**, 307, 435–446.
8- E. çAğLar, Y. O. Donar, A. Sinağ, İ. Biroğul, S. Bilge, K. Aydincak, O. Pliekhov, Adsorption of anionic and cationic dyes on biochars, produced by hydrothermal carbonization of waste biomass: effect of surface functionalization and ionic strength," Turkish Journal of Chemistry, **2018**, 42, 86–99.
9- S. Zhang, Z. Wang, Y. Zhang, H. Pan, and L. Tao, Adsorption of Methylene Blue on Organosolv Lignin from Rice Straw, Procedia Environmental Science, **2016**, 31, 3-11.
10- S. Shakoor and A. Nasar, Adsorptive treatment of hazardous methylene blue dye from artificially contaminated water using cucumis sativus peel waste as a low-cost adsorbent, Groundwater for Sustainable Development, **2017**, 5, 152–159.
11- S. Rangabhashiyam, S. Lata, P. Balasubramanian, Biosorption characteristics of methylene blue and malachite green from simulated wastewater onto Carica papaya wood biosorbent, *Surfaces and Interfaces*, **2018**, 10, 197-215.
12- A. Aarfane, A. Salhi, M. El Krati, S. Tahiri, M. Monkade, E. K. Lhadi, M. Bensitel, Kinetic and thermodynamic study of the adsorption of Red195 and Methylene blue dyes on fly ash and bottom ash in aqueous medium, Journal of Material and Environmental Sciences, **2014**, 5, 1927–1939.
13- F. Sakr, A. Sennaoui, M. Elouardi, M. Tamimi, A. Assabbane, Adsorption study of Methylene Blue on biomaterial using cactus, Journal of Material and Environmental Sciences , **2015**, 6, 397–406.
14- A. Sarimeseli, Microwave drying characteristics of coriander (Coriandrum sativum L.) leaves, Energy Conversion and Management, **2011**, 52, 1449–1453.
15- K. Msaada, M. Ben Jemia, N. Salem, O. Bachrouch, J. Sriti, S. Tammar, I. Bettaieb, Antioxidant activity of methanolic extracts from three coriander (Coriandrum sativum L.) fruit varieties, Arabian Journal of Chemistry, **2013**, 10, S3176-S3183.
16- H. Wangensteen, A. B. Samuelsen, K. E. Malterud, Antioxidant activity in extracts from coriander, Food Chemistry, **2004**, 88, 293–297.
17- P. J. Delaquis, K. Stanich, B. Girard, G. Mazza, Antimicrobial activity of individual and mixed fractions of dill, cilantro, coriander and eucalyptus essential oils, International Journal of Food and Microbiology. **2002**, 74, 101–109.
18- S. Mandal, M. Mandal, Coriander (Coriandrum sativum L.) essential oil: Chemistry and biological activity, Asian Pacific Journal of Tropical Biomedicine **2015**, 5, 421–428.
19- V. Chithra, S. Leelamma, Coriandrum Sativum-mechanism of hypoglycemic action, Food Chemistry. **1999**, 67, 229–231.
20- L. Kadiri, M. Galai, M. Ouakki, Y. Essaadaoui, A. Ouass, M. Cherkaoui, E. H. Rifi, A. Lebkiri, Coriandrum Sativum.L Seeds Extract as a Novel Green Corrosion Inhibitor for Mild Steel in 1.0 M Hydrochloric and 0.5 M Sulfuric Solutions, Analytical and Bioanalytical Chemistry, **2018**, 10, 249–268.
21- L. Kadiri, A. Lebkiri, E. H. Rifi, A. Ouass, Y. Essaadaoui, I. Lebkiri, H. Hamad, Kinetic studies of adsorption of Cu (II) from aqueous

solution by coriander seeds (Coriandrum Sativum), E3S Web of conferences. **2018**, 37, 02005.

22- L. Kadiri, A. Lebkiri, E. H. Rifi, A. Ouass, Y. Essaadaoui, I. Lebkiri, H. Hamad, Characterization of coriander seeds “Coriandrum Sativum”, *International Journal of Sciences, Engineering and Research*. **2017**, 8, 2303-2308.

23- A. Khodabandehloo, A. Rahbar-Kelishami, H. Shayesteh, Methylene blue removal using Salix babylonica (Weeping willow) leaves powder as a low-cost biosorbent in batch mode: Kinetic, equilibrium, and thermodynamic studies, Journal of Molecular Liquids, **2017**, 244, 540–548.

24- V. K. Gupta, A. Mittal, V. Gajbe, J. Mittal, Removal and Recovery of the Hazardous Azo Dye Acid Orange 7 through Adsorption over Waste Materials: Bottom Ash and De-Oiled Soya, *Industrial & Engineering Chemistry Research*, **2006,** 45, 1446–1453.

25- A. K. Nayak and A. Pal, Green and efficient biosorptive removal of methylene blue by Abelmoschus esculentus seed: Process optimization and multi-variate modeling, Journal of Environmental Management, **2017**, 200, 145-159.

26- F. Bouaziz, M. Koubaa, F. Kallel, F. Chaari, D. Driss, R. E. Ghorbel, S. E. Chaabouni, Efficiency of almond gum as a low-cost adsorbent for methylene blue dye removal from aqueous solutions, Industrial Crops and Products, **2015**, 74, 903-911.

27- Y. Essaadaoui, A. Lebkiri, E. H. Rifi, L. Kadiri, A. Ouass, Adsorption of cobalt from aqueous solutions onto Bark of Eucalyptus. Mediterr.J.Chem., **2018**, 7(2), 145-155.

28- J. Pang, F. Fu, Z. Ding, J. Lu, N. Li, B. Tang, Adsorption behaviors of methylene blue from aqueous solution on mesoporous birnessite, Journal of the Taiwan Institute of Chemical Engineers, **2017**, 77, 168-176.

29- A. Abdallah, A. Hijazi, M. Hamieh, M. Alameh, J. Toufaily, H. Rammal, Treatment of industrial wastewater using a natural and biodegradable adsorbent based on Eucalyptus, Journal of Material and Environmental Sciences. **2016**, 5, 4036–4048.

30- M. Basu, A. K. Guha, and L. Ray, Adsorption of Lead on Cucumber Peel, Journal of Cleaner Production, **2017**, 151, 603–615.

31- M. Basu, A. K. Guha, and L. Ray, Biosorptive removal of lead by lentil husk, Journal of Environmental Chemical Engineering, **2015**, 3, 1088–1095.

32- Y. Essaadaoui, A. Lebkiri, E. H. Rifi, L. Kadiri, A. Ouass, Adsorption of lead by modified Eucalyptus camaldulensis barks: equilibrium, kinetic and thermodynamic studies, Desalination and water treatment. **2018**, 111, 267-277.

33- K. Z. Elwakeel, A. M. Elgarahy, S. H. Mohammad, Use of beach bivalve shells located at Port Said coast (Egypt) as a green approach for methylene blue removal, Journal of Environmental Chemical Engineering. **2017**, 5, 578-587.

34- A. K. Agarwal, M. S. Kadu, kinetics study on the adsorption of Ni^{2+} ions onto fly ash, Journal of Chemical Technology and Metallurgy, **2015**, 50, 601-605.

35- I. Langmuir, The constitution and fundamental properties of solids and liquids. Part I. Solids, Journal of the American chemical society, **1917**, 39, 1848–1906

36- A. Ouass, I. Ismi, H. Elaidi, A. Lebkiri, M. Cherkaoui, E. H. Rifi, Mathematical Modeling Of The Adsorption Of Trivalent Chromium By The Sodium Polyacrylate Beads, Journal of Material and Environmental Sciences, **2017**, 8, 3448–3456.

37- B. Xu, Y. Zhu, H. Liu, Z. Jin, T. Chen, The kinetic and thermodynamic adsorption of Eu(III) on synthetic maghemite, Journal of Molecular Liquids, **2016**, 221, 171–178.

38- C. S. T. Araújo, I. L. S. Almeida, H. C. Rezende, S. M. L. O. Marcionilio, J. J. L. Léon, T. N. de Matos, Elucidation of mechanism involved in adsorption of Pb(II) onto lobeira fruit (Solanum lycocarpum) using Langmuir, Freundlich and Temkin isotherms, Microchemical Journal, **2018**, 137, 348–354.

39- T. Liu, Y. Li, Q. Du, J. Sun, Y. Jiao, G. Yang, Z. Wang, Y. Xia, W. Zhang, K. Wang, H. Zhu, D. Wu, Adsorption of methylene blue from aqueous solution by graphene. Colloids and Surfaces B: Biointerfaces, **2012**, 90, 197-203.

40- P. Joshi, S. Manocha, Kinetic and thermodynamic studies of the adsorption of copper ions on hydroxyapatite nanoparticles, Materials Today: Proceedings. **2017**, 4, 10455–10459.

41- X. Liu, D.-J. Lee, Thermodynamic parameters for adsorption equilibrium of heavy metals and dyes from wastewaters, Bioresource Technol. **2014**, 160, 24–31.

42- A. Ouass, L. Kadiri, Y. Essaadaoui, R. A. Belakhmima, M. Cherkaoui, A. Lebkiri, E. H. Rifi, Removal of trivalent chromium ions from aqueous solutions by Sodium polyacrylate beads. Mediterr.J.Chem., **2018**, 7(2), 125-134.

43- C. C. Okoye, O. D. Onukwuli, C. F. Okey-Onyesolu, Utilization of salt activated Raphia hookeri seeds as biosorbent for Erythrosine B dye removal: Kinetics and thermodynamics studies, Journal of King Saud University, **2018**, DOI: https://doi.org/10.1016/j.jksus.2017.11.004.